Letter

Time-reversal symmetry breaking in the superconducting low carrier density quasiskutterudite $Lu_3Os_4Ge_{13}$

A. Kataria,[1] J. A. T. Verezhak,[2] O. Prakash,[3] R. K. Kushwaha,[1] A. Thamizhavel,[3] S. Ramakrishnan,[3] M. S. Scheurer,[4] A. D. Hillier,[5] and R. P. Singh[1,*]

[1]*Department of Physics, Indian Institute of Science Education and Research Bhopal, Bhopal 462066, India*
[2]*Department of Physics, University of Warwick, Coventry CV4 7AL, United Kingdom*
[3]*Department of Condensed Matter Physics and Materials Science, Tata Institute of Fundamental Research, Mumbai-400005, India*
[4]*Institute for Theoretical Physics, University of Innsbruck, A-6020 Innsbruck, Austria*
[5]*ISIS Facility, STFC Rutherford Appleton Laboratory, Didcot OX11 0QX, United Kingdom*

(Received 4 November 2022; revised 9 March 2023; accepted 17 March 2023; published 30 March 2023)

The complex structure of the Remeika phases, the intriguing quantum states they display, and their low carrier concentrations are strong motivations to study the nature of their superconducting phases. In this Letter, the microscopic properties of the superconducting phase of single-crystalline $Lu_3Os_4Ge_{13}$ are investigated by muon-spin relaxation and rotation (μSR) measurements. The zero-field μSR data reveal the presence of spontaneous static or quasistatic magnetic fields in the superconducting state, breaking time-reversal symmetry; the associated internal magnetic-field scale is found to be exceptionally large ($\simeq 0.11$ mT). Furthermore, transverse-field μSR measurements in the vortex state of $Lu_3Os_4Ge_{13}$ imply a complex gap function with significantly different strengths on different parts of the Fermi surface. Although our measurements do not completely determine the order parameter, they strongly indicate that electron-electron interactions are essential to stabilizing pairing in the system, thus, demonstrating its unconventional nature.

DOI: 10.1103/PhysRevB.107.L100506

Introduction. Intriguing phenomena, such as non-Fermi-liquid behavior, spin or charge order, nontrivial band topology, and a complex crystal structure, often accompany unconventional pairing mechanisms and nontrivial, symmetry-breaking superconducting order parameters in phase diagrams. The Remeika 3-4-13 series is an example of a family of materials, which exhibits a wide array of diverse, exotic phenomena [1–4], and exciting properties, including the Kondo effect, spin-fluctuation superconductivity, multigap superconductivity, and many more [5–7]. The Remeika phase has the form $R_3A_4X_{13}$, where R is a rare-earth metal, A is a transition metal, and X is a group-14 element [8], and its structure motif is isomorphic to cagelike compounds, namely, clathrates and filled skutterudites; thus, the name quasiskutterudites [9,10]. The stannides of the 3-4-13 family are believed to be strongly coupled superconductors with a second-order structural phase transition, pointing towards a strong interplay between the superconducting order and their structures [2,11–15]. Meanwhile, germanides $R_3A_4Ge_{13}$, which are similar to the stannide structure, are scarce and mostly uninvestigated. A number of germanide compounds exhibit low-temperature superconductivity and paramagnetic character different from the stannides [16,17]; thus, presenting an interesting platform in the 3-4-13 family to inspect the connection between crystal complexity and superconductivity.

In the 3-4-13 germanides family, $Lu_3Os_4Ge_{13}$, a semimetallic compound, has shown interesting properties in the superconducting state and attracted attention recently. Two initial studies of $Lu_3Os_4Ge_{13}$ by Prakash *et al.* revealed multigap bulk superconductivity from specific-heat measurements and a nonlinear dependence of the Sommerfeld coefficient γ_n under a magnetic field [18,19]. The superfluid density measurements via tunnel diode oscillator (TDO) also confirmed the two-gap nature of the superconducting state [20]. Another noteworthy property of $Lu_3Os_4Ge_{13}$ is the high value of the upper critical field H_{c2} close to its Pauli limiting value [21], and the high transition temperature T_c for a relatively low carrier density of the system. Other low-carrier density systems with high T_c include cuprates, fullerenes, and MgB_2, which are known for their fascinating properties [22–24]. Exploring the phenomenology of low carrier density superconductors is also crucial for our theoretical understanding as the conventional BCS theory is not applicable to the low-density limit. This motivates a detailed microscopic investigation of the germanide superconductor $Lu_3Os_4Ge_{13}$ in order to understand its superconducting order parameter, the pairing mechanism, and their relation with the structure.

Moreover, other cage-type structure systems, such as $R_5Rh_6Sn_{18}$ (R = Sc, Lu, and Y) and Pr-based heavy-fermion skutterudite $(Pr,La)(Ru,Os)_4Sb_{12}$, $PrPt_4Ge_{12}$ are among the few compounds which show time-reversal symmetry breaking (TRSB) in their superconducting state with multigap features [25–30]. This further motivates a detailed study of the pairing symmetry in the quasiskutterudite $Lu_3Os_4Ge_{13}$, which

*rpsingh@iiserb.ac.in

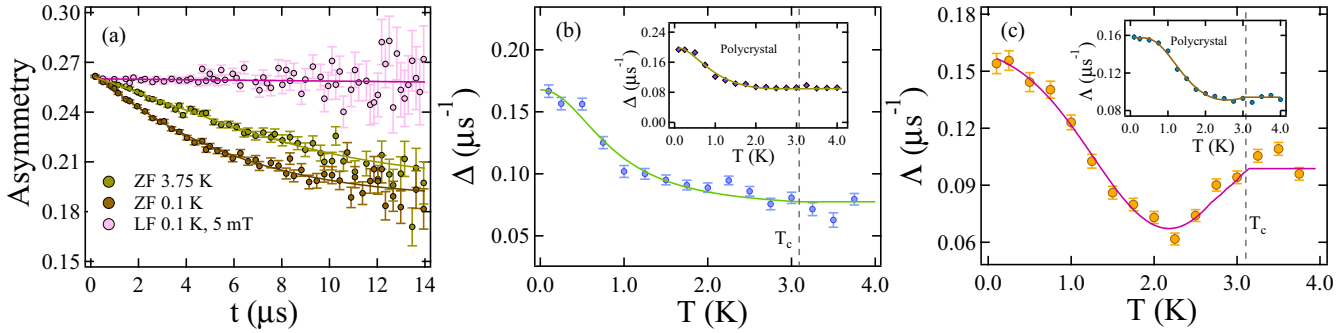

FIG. 1. (a) ZF-μSR spectra for single-crystalline $Lu_3Os_4Ge_{13}$ at a temperature above (green color) and below (brown color) T_c with the LF-μSR spectra in an applied field of 5 mT at 0.1 K. The temperature variation of (b) Δ and (c) Λ estimated by fitting Eqs. (1) and (2); the inset of the two represents the same relaxation variation for the polycrystalline sample.

exhibits analogous cage-type structure with multigap superconductivity and structural complexity.

In this Letter, the superconducting state of $Lu_3Os_4Ge_{13}$ is investigated microscopically, using muon spin rotation and relaxation measurements (μSR). Zero-field (ZF) μSR reveal a significant variation of the relaxation rate with temperature and, thus, the presence of spontaneous magnetic fields, breaking time-reversal symmetry in the superconducting state. Furthermore, transverse-field (TF) measurements of $Lu_3Os_4Ge_{13}$ provide the temperature dependence of the superconducting contribution to the relaxation rate σ_{sc}, which is in accordance with the previous reports [19,20]—is consistent with a multigap state with significantly different gap magnitude on different Fermi sheets. We find comparatively small values of $\Delta_i(T=0)/k_BT_c$ for the two superconducting gaps Δ_i, indicative of weakly coupled superconductivity in $Lu_3Os_4Ge_{13}$.

Experimental details. μSR measurements were conducted on both single and polycrystalline samples of $Lu_3Os_4Ge_{13}$, which have previously been characterized and studied as a superconductor with $T_c = 3.1$ K in Refs. [18,19]. The μSR measurements were carried out using various configurations, including ZF, longitudinal-field (LF), and TF modes, utilizing the μSR spectrometer at the ISIS Neutron and Muon Pulsed Source located in the Appleton Laboratory, UK [31,32]. For all measurements, single crystals oriented in one of the principal axes [100] are used, and the incident muon beam is always perpendicular to the [100] plane of the crystal. In TF measurements, the magnetic field is applied perpendicular to the muon spin direction and [100] crystal axis (i.e., parallel to the [100] crystal plane). Furthermore, for LF measurements, the field was perpendicular to the [100] crystal plane.

Results. a. Zero-field μSR. The ZF asymmetry spectra above and below the superconducting transition temperature, together with the LF spectra at 0.1 K and 5 mT magnetic field for single-crystalline $Lu_3Os_4Ge_{13}$ are shown in Fig. 1(a). A significant change in the relaxation rate from the superconducting (0.1 K) to the normal state (3.75 K) is observed with no oscillating signal, which directs toward the possible presence of a spontaneous magnetic field below the superconducting transition temperature. For static randomly oriented nuclear moments, the asymmetry spectra can be understood from the Gaussian Kubo-Toyabe equation [33],

$$G_z(t) = \frac{1}{3} + \frac{2}{3}(1-\Delta^2t^2)\exp\left(-\frac{\Delta^2t^2}{2}\right), \tag{1}$$

where Δ corresponds to relaxation due to the dipolar nuclear field. The measured time-dependent ZF asymmetry spectra are well described by the muon relaxation function [34],

$$A(t) = A_0G_z(t)\exp(-\Lambda t) + A_{bg}, \tag{2}$$

where A_0 is the initial asymmetry corresponding to the sample, A_{bg} considers the background asymmetry, and Λ accounts for the electronic relaxation rate. The temperature dependence of the relaxation rates (i.e., the fitting parameters) Δ and Λ for single-crystalline $Lu_3Os_4Ge_{13}$ are shown in Figs. 1(b) and 1(c) where the sample and background asymmetries are temperature independent. A significant variation in Λ and Δ is observed below the transition temperature. The insets of Figs. 1(b) and 1(c) depict the similar variation of relaxation rates for the polycrystalline sample. Both poly and single-crystalline data complement each other; however, in the polycrystalline sample, the dip feature in Δ is suppressed, and only a small variation around the dip temperature is observed.

The increment nature of relaxation rates Λ and Δ with temperature [Figs. 1(b) and 1(c)], can be attributed to either fast fluctuations arising from electronic spins or the presence of static or quasistatic magnetic fields in the sample below the superconducting transition temperature. Considering the case of relaxation due to fluctuations, the field fluctuations perpendicular to the applied field can cause spin-flip transitions of the muon spin, which leads to an overall relaxation of the muon ensemble and a Curie-Weiss-like temperature dependence [35]. Furthermore, the slow-time evolution of LF asymmetry spectra [Fig. 1(a)], i.e., the low relaxation rate, indicates the decoupling of muon spin from the local magnetic-field environment even with an applied magnetic field as low as 5 mT. This implies that the observed signal of increased relaxation rate with temperature is emerging from a dilute static or quasistatic magnetic field in the system, breaking time-reversal symmetry and excluding the possibility of any extrinsic magnetic impurity effects in $Lu_3Os_4Ge_{13}$. Such a change in Λ below T_c has only been observed in a limited

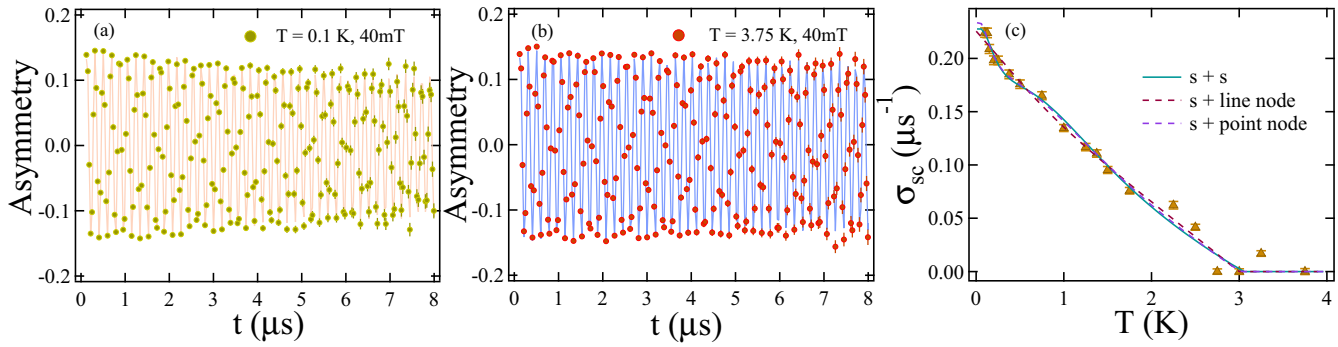

FIG. 2. TF-μSR spectra at 40 mT fields (a) below (superconducting state) and (b) above (normal state) the transition temperature. (c) The superconducting relaxation rate σ_{sc} variation with the temperature where the solid cyan line, pink dotted line, and purple dotted line represent the (a) $s+s$, (b) $s+$ line and, (c) $s+$ point node, respectively.

superconductors, including Sr_2RuO_4 [36], $LaNiC_2$ [37], SrPtAs [38], $(Lu/Y/Sc)_5Rh_6Sn_{18}$ [25–27], $Ba_{1-x}K_xFe_2As_2$ [39], La_7X_3 (X = Rh, Ir, Pd, and Ni) [40–43] series and recently in monochalcogenide ScS [44]. Furthermore, the relaxation channel Δ represents the width of the dipolar nuclear field of the atoms and exhibits a variation in the low-temperature region significantly below T_c. The temperature evolution of Δ is likely due to Lu atoms having the largest nuclear moment among the three constituent atoms. Meanwhile, the relatively small increment of Δ compared to Λ makes it a secondary channel of the muon relaxation. The change in the secondary channel with TRSB is also observed in La_7Ir_3, La_7Pd_3, La_7Rh_3 [41–43], and $Pr_{1-x}La_xPt_4Ge_{12}$, $Pr(Os_{1-x}Ru_x)_4Sb_{12}$, $Pr_{1-y}La_yOs_4Sb_{12}$ [29,45]. For the aforementioned materials, the proposed reason for the increment in the secondary channel (mainly Λ) is nuclear spin fluctuations. However, this is not particularly associated with an increase in Δ. The net change observed in the secondary channel is much lower than the value in Δ for our single-crystalline $Lu_3Os_4Ge_{13}$. The underlying cause of our system's low-temperature increment of Δ is unknown.

The value of a static or quasistatic magnetic field in the sample below the transition temperature is evaluated from the observed change in Λ. Subtracting the minimum value of Λ to its maximum value at the lowest temperature yields the net increase $\delta\Lambda = 0.094\ \mu s^{-1}$. The characteristic local magnetic-field strength can be estimated from $\delta\Lambda/\gamma_\mu = B_{\rm loc}$, providing $B_{\rm loc} \simeq 0.11$ mT [46]. The observed local field strength is much larger than the values reported for the other TRSB compounds in their superconducting state (e.g., for Sr_2RuO_4 it is 0.05 mT [36]) but comparable to the value reported for the skutterudite and the frustrated superconductor (0.12 mT for $PrOs_4Sb_{12}$ and 0.116 mT for Re_2Hf [28,47]).

Notably, the increment in electronic relaxation rate Λ is observed at a temperature different from T_c, defined as the onset temperature of TRSB, $T_{\rm onset} = 2.2$ K. With increasing temperature, a small diplike feature in the Λ is followed by the constant value above the transition temperature. The similar diplike feature in the relaxation channel with two temperatures, $T_{\rm onset}$ and T_c, are also observed in the other TRSB skutterudite superconductors, such as $PrPt_4Ge_{12}$ [30], $Pr_{1-x}Ce_xPt_4Ge_{12}$ [48], $Pr_{1-x}La_xPt_4Ge_{12}$ [45] and recently in La_7Ni_3 [40]. However, the dip reason is unknown and is believed to be associated with the multicomponent nature of the superconducting order parameter. This is discussed later for our case of quasiskutterudite $Lu_3Os_4Ge_{13}$.

b. Transverse-field μSR. The asymmetry spectra in the TF configuration above and below the transition temperature T_c under an applied magnetic field of 40 mT for single-crystalline $Lu_3Os_4Ge_{13}$ are shown in Figs. 2(a) and 2(b). The decay in asymmetry spectra amplitude below T_c reveals the presence of the inhomogeneous field distribution in the flux-line lattice. To this end, the time-domain asymmetry spectra are described by a Gaussian-damped oscillatory muon spin relaxation function [49,50],

$$A(t) = \sum_{i=1}^{N} A_i \exp\left(-\frac{1}{2}\sigma_i^2 t^2\right)\cos(\gamma_\mu B_i t + \phi), \qquad (3)$$

where A_i and σ_i are the corresponding initial asymmetry and Gaussian relaxation rate, respectively. ϕ is the offset phase, and B_i is the $i^{\rm th}$ component of the magnetic-field distribution with $\gamma_\mu/2\pi = 135.5$ MHz/T being the muon gyromagnetic ratio. Here, $N = 2$ describes the distribution appropriately with σ_2 fixed to zero to account for the nondepolarizing background originating from the sample holder. Thus, A_2 and B_2 correspond to the background asymmetry and magnetic field, respectively.

The extracted temperature-dependent total Gaussian relaxation rate, σ consists of a contribution from both the flux-line lattice (σ_{sc}) and nuclear moment (σ_n). A temperature-invariant relaxation rate from the nuclear moment σ_n is obtained from the asymmetry spectra measured above T_c. Thus, the superconducting contribution of the relaxation rate is evaluated via $\sigma_{sc}=\sqrt{\sigma^2 - \sigma_n^2}$. For a vortex lattice system having $\kappa \geqslant 5$ and an applied field much smaller than the upper critical field ($H_{\rm app} \ll H_{c2}$), the relation of σ_{sc} and effective magnetic penetration depth $\lambda_{\rm eff}$ reads as [51]

$$\frac{\sigma_{sc}(T)}{\gamma_\mu} = 0.0609\frac{\Phi_0}{\lambda_{\rm eff}^2(T)}, \qquad (4)$$

where Φ_0 is the magnetic flux quantum. Hence, σ_{sc} provides information on the superconducting gap structure. From the above expression, the estimated value of $\lambda_{\rm eff}(0) = 691(13)$ nm. Using the definition of λ_0, the fundamental finding of BCS and Ginzburg-Landau theory [52,53] and the expressions in Refs. [18,19,54], the ratio of BCS coherence length and mean free path, $\xi_0/l = 9.25(5)$ is extracted. Furthermore, the dirty-limit relation of $\lambda_{\rm eff}$ and London's penetration depth, λ_L and London's equation $\lambda_L^2 = m^*/\mu_0 n_s e^2$

TABLE I. Summary of two superconducting gap analyses for single-crystalline $Lu_3Os_4Ge_{13}$ via various models from different studies (indicated in the last column), including our TF-μSR, specific-heat (SH), and TDO measurements.

Model	χ^2	T_c	Fraction (w_1)	$\Delta_{0,1}$ (meV)	$\Delta_{0,2}$ (meV)	$\Delta_{0,1}/\Delta_{0,2}$	Measurement	Reference
$s+s$	1.36	3.0(1)	0.27(4)	0.04(1)	0.30(2)	7.5	TF	This Letter
$s+$ point	1.37	3.0(1)	0.24(7)	0.03(1)	0.37(3)	12.3	TF	This Letter
$s+$ line	1.38	3.0(1)	0.3(2)	0.6(1)	1.4(4)	4.6	TF	This Letter
$s+s$	1.31	3.1	0.18	0.04(3)	0.43(1)	10.8	SH	[19]
$s+s$		3.0	0.22	0.33	0.65	1.9	TDO	[20]

are used to extract the carrier density n_s where m^* is the effective mass [19]. The resultant superconducting carrier density is $n_s = 9.5(4) \times 10^{26}$ carriers/m^3.

The increase in σ_{sc} with decreasing temperature is ascribed to the development of the vortex lattice as the superconductor enters the mixed phase. In Fig. 2(c), σ_{sc} versus T curve is shown where the superconducting transition appears to be very broad. The curve depicts an approximately linear behavior down to very low temperature and without any saturation features; this indicates nodal pairing or multiple superconducting gaps with significantly different magnitudes ruling out a single isotropic gap. To be more quantitative, the σ_{sc} temperature evolution can be presented in the semiclassical approximation as [55,56]

$$\delta\sigma_{sc}(T, \Delta_{0,i}) = 1+2\left\langle \int_{\Delta(T,\phi,\theta)}^{\infty} \frac{\delta f}{\delta E} \frac{EdE}{\sqrt{E^2-|\Delta_i(T,\phi,\theta)|^2}} \right\rangle_{\mathrm{FS}}, \tag{5}$$

here $f(E) = [\exp(E/k_BT)+1]^{-1}$ is the Fermi-Dirac function and $\langle\cdots\rangle_{\mathrm{FS}}$ represents the average over the Fermi surface. The gap function $\Delta_i(T,\phi,\theta)$ consists of the product $\Delta_i(T/T_c)g(\phi,\theta)$ with $g(\phi,\theta)$ encoding the angular dependence of the gap around the Fermi surface at an azimuthal angle ϕ and polar angle θ. We use [57]

$$\Delta_i(T/T_c) = \Delta_{0,i}\tanh\left\{1.82\left[1.018\left(\frac{T_c}{T}-1\right)\right]^{0.51}\right\}, \tag{6}$$

with $\Delta_{0,i}$ being the gap value at $T = 0$, which approximates the BCS temperature dependence of $\Delta_i/\Delta_{0,i}$ well. To account the experimental data quantitatively, various two-gap scenarios based on the α model [58,59] are applied: (a) a fully gapped $s+s$ state, (b) a model with a full gap on one and with nodal lines on the second Fermi sheet (denoted by the $s+$ line), and (c) a full gap on one and point nodes on the second sheet ($s+$ point). For the full gap, line nodes, and point nodes, we use $g(\phi,\theta) = 1$, $g(\phi,\theta) = |\cos(2\phi)|$, and $g(\phi,\theta) = |\sin\theta|$, respectively. The two-gap model is incorporated by using a weighted sum of two gap values as [40,60,61]

$$\frac{\sigma_{sc}(T)}{\sigma_{sc}(0)} = w_1\delta\sigma_{sc}(T,\Delta_{0,1}) + w_2\delta\sigma_{sc}(T,\Delta_{0,2}), \tag{7}$$

where w_1 and w_2 are the weighting fractions of their superconducting gap $\Delta_{0,1}$ and $\Delta_{0,2}$ with $w_1+w_2 = 1$. The two-gap model describes the data well but requires significantly different gap magnitudes $\Delta_{0,1}$ and $\Delta_{0,2}$. For instance, the $s+s$ model yields $\Delta_{0,1}(0) = 0.04(1)$ meV and $\Delta_{0,2}(0) = 0.30(2)$ meV with $w_1 = 0.27(4)$. The obtained value from the $s+s$-wave model with the lowest χ^2 value agrees with the two-gap values stated from the specific-heat data but deviates from the superfluid density measurement values [20]. The superconducting gap analysis of $Lu_3Os_4Ge_{13}$ is summarized in Table I with the observed values from other studies. The variation in gap values via different techniques might be due to the incorporation of various assumptions in the calculations. In addition, we attempted to fit the temperature variation of σ_{sc} using the dirty limit model [62], finding that the clean and dirty limit fits are indistinguishable and both fit the data well.

Importantly, since the χ^2 values for the other two-gap models we investigated, the $s+$ line and the $s+$ point nodes are close, our data do not allow us to distinguish between nodal multiband pairing and fully gapped multigap behavior with strongly varying gap magnitude (near nodal). We note that multigap behavior is natural for a system, such as $Lu_3Os_4Ge_{13}$ with several complex Fermi surfaces as revealed by first-principle band structure calculations [19] and is also evident from various experimental observations [19,20]. The low dimensionless gap values of $\Delta_{0,i}/k_BT_c$ obtained for $Lu_3Os_4Ge_{13}$ ($\simeq 1.1, 0.15$) are counter to those of the stannides where values above that of the BCS theory have been observed [63].

Discussion. $Lu_3Os_4Ge_{13}$ crystallizes in the space-group $Pm\bar{3}n$ (No. 223) with point-group O_h. If the superconducting phase in the system is reached by a single continuous phase transition, we know that the pairing state must transform under one of the irreducible representations (IRs) of O_h (setting aside rather exotic scenarios where its order parameter transforms nontrivially under lattice translations). In total, O_h has ten IRs, some of which are two or even three dimensional, leading to 26 possible superconducting instabilities [64]. Our ZF-μSR measurements, however, indicate TRSB superconductivity, which strongly constrains the order parameter symmetries: first, time-reversal symmetry can only be broken at a single superconducting transition if the order parameter transforms under a multidimensional IR. In our case, this leaves us with the six IRs E_μ, $T_{1\mu}$, and $T_{2\mu}$, $\mu = g, u$. Furthermore, only some states transforming under these IRs will break time-reversal symmetry; a systematic analysis shows [64] that there are ten such TRSB superconductors. Interestingly, symmetry implies that all of these states will either have nodal points or lines on some of the Fermi sheets [19]. As already pointed out above [cf. Fig. 2(c) and Table I], our TF-μSR results are not incompatible with the nodes in the superconducting states. Recall, although, that a fully gapped $s+s$ state is also consistent with our TF-μSR data, albeit with significantly different gap magnitude on different Fermi surfaces in order to reproduce the seemingly nonexponential behavior of σ_{sc} at low T in Fig. 2(c). In combination with the fact that previous TDO measurements [20] found exponential

low-T behavior of the penetration depth of $Lu_3Os_4Ge_{13}$, we here also discuss how full-gap superconductivity could be reconciled with broken time-reversal symmetry. The above discussion of pairing states makes the simplifying assumption that the TRSB superconductor is reached via a single transition. On one hand, this is natural since we currently do not have any clear indications of several transitions close to T_c; if there are two different T_c's, they are not resolved by the TF measurements [Fig. 2(c)]. On the other hand, the fact that Λ in Fig. 1(c) only increases at a temperature that is significantly smaller than T_c might point towards the following scenario: right at T_c as identified in transport, a first superconducting order parameter sets in; it does not break time-reversal symmetry and may or may not be fully gapped. At a temperature lower than T_c, a secondary order parameter sets in and time-reversal symmetry is broken, e.g., due to some nontrivial complex phase between the primary and the secondary order parameter, which leads to spontaneous fields [65]. In this way, one can obtain a fully gapped TRSB superconductor. The simplest such scenario is an $s + is$ state where both superconducting components are trivial under O_h (IR A_{1g}) and, hence, generically fully gapped. The relative complex phase can arise from "frustrated" Cooper-channel interactions between the different pockets of the system; see, e.g., Ref. [40] for an illustration in a toy model or Ref. [66]. Another more complex scenario is that the primary and secondary order parameters are even and odd in frequency. As recently pointed out in Ref. [67], this can be realized for strong electron-phonon coupling, competing with Coulomb repulsion, if the phonon and Fermi energy scales become comparable. Due to the low carrier concentrations in superconducting $Lu_3Os_4Ge_{13}$ [21], this scenario does not seem implausible either.

We emphasize that all of the above scenarios require a repulsive Coulomb interaction on top of electron-phonon coupling to stabilize the pairing phase. As such, our data clearly indicate the presence of an unconventional pairing mechanism in $Lu_3Os_4Ge_{13}$. Together with the multigap and the multiband nature as well as the low-carrier concentration, this makes $Lu_3Os_4Ge_{13}$ an exciting system to study pairing beyond the BCS paradigm.

Summary and conclusions. In conclusion, the microscopic properties of the superconducting state are investigated for the low-carrier, quasiskutterudite $Lu_3Os_4Ge_{13}$. The ZF-μSR data indicate spontaneous time-reversal-symmetry breaking in the superconducting state, reflected by the increase in relaxation rate Λ in Fig. 1(c) at a temperature, $T_{\text{onset}} \simeq 2.2$ K, below the superconducting transition temperature $T_c \simeq 3.1$ K. The measured strength of the dilute magnetic field in the superconducting state of $Lu_3Os_4Ge_{13}$ is $\simeq 0.11$ mT—a value much larger than that of most TRSB superconductors, whereas only those of $PrOs_4Sb_{12}$ and Re_2Hf are comparable [28,47]. The variation of σ_{sc} with temperature, extracted from our TF measurements, is inconsistent with a single isotropic pairing state. Meanwhile, it is well described by a two-gap scenario with large gap anisotropy $\Delta_{0,1}/\Delta_{0,2} \simeq 5$–12, in accordance with previous studies [19,20] and with the presence of multiple bands at the Fermi level [19]; we emphasize that our data is consistent with both fully gapped and nodal states, see Table I and Fig. 2(c). A symmetry analysis of pairing states shows that reaching a TRSB superconducting state in $Lu_3Os_4Ge_{13}$ via a single continuous phase transition is only consistent with the latter nodal-pairing scenario. However, a full-gapped TRSB state could be naturally reached via two consecutive transitions.

Taken together, our findings establish $Lu_3Os_4Ge_{13}$ as an exciting superconducting compound that combines not only pairing at low-carrier concentrations and multiple bands, but also spontaneous symmetry breaking in the superconducting state and unconventional pairing mechanisms. More theoretical and experimental work is required on $Lu_3Os_4Ge_{13}$, in particular, and Remeika phase germanides, in general, to identify the complex microscopic physics in these systems.

Acknowledgments. A.K. acknowledges the funding agency Council of Scientific and Industrial Research (CSIR), Government of India, for a SRF Fellowship (Award No: 09/1020(0172)/2019-EMR-I). R.P.S. acknowledges Science and Engineering Research Board, Government of India, for the CRG/2019/001028 Core Research Grant. M.S.S. acknowledges funding by the European Union (ERC-2021-STG, Project No. 101040651—SuperCorr). Views and opinions expressed are, however, those of the authors only and do not necessarily reflect those of the European Union or the European Research Council Executive Agency. Neither the European Union nor the granting authority can be held responsible for them.

[1] R. Gumeniuk, in *The Physics and Chemistry of Rare Earths* (Elsevier, Amsterdam, 2018), p. 54.

[2] L. E. Klintberg, S. K. Goh, P. L. Alireza, P. J. Saines, D. A. Tompsett, P. W. Logg, J. Yang, B. Chen, K. Yoshimura, and F. M. Grosche, Phys. Rev. Lett. **109**, 237008 (2012).

[3] A. M. Hallas, C. L. Huang, B. K. Rai, A. Weiland, G. T. McCandless, J. Y. Chan, and E. Morosan, Phys. Rev. Mater. **3**, 114407 (2019).

[4] O. Prakash, A. Thamizhavel, and S. Ramakrishnan, Phys. Rev. B **93**, 064427 (2016).

[5] S. Y. Zhou, H. Zhang, X. C. Hong, B. Y. Pan, X. Qiu, W. N. Dong, X. L. Li, and S. Y. Li, Phys. Rev. B **86**, 064504 (2012).

[6] C. L. Yang, X. Wang, X. Zhang, D. S. Wu, M. Liu, P. Zheng, J. Y. Yao, Z. Z. Li, Y.-F. Yang, Y. G. Shi, J. L. Luo, and N. L. Wang, Phys. Rev. B **91**, 075120 (2015).

[7] P. K. Biswas, A. Amato, R. Khasanov, H. Luetkens, K. Wang, C. Petrovic, R. M. Cook, M. R. Lees, and E. Morenzoni, Phys. Rev. B **90**, 144505 (2014).

[8] J. P. Remeika, G. P. Espinosa, A. S. Cooper, H. Barz, J. M. Rowell, D. B. McWhan, J. M. Vandenberg, D. E. Moncton, Z. Fisk, L. D. Woolf, and H. C. Hamaker, Solid State Commun. **34**, 923 (1980).

[9] K. A. Kovnir and A. V. Shevelkov, Russ. Chem. Rev. **73**, 923 (2004).

[10] K. A. Gschneidner, J. C. G. Bunzli, and V. K. Pecharsky, *Handbook on the Physics and Chemistry of Rare Earths* (Elsevier, Amsterdam, 2004).

[11] S. K. Goh, D. A. Tompsett, P. J. Saines, H. C. Chang, T. Matsumoto, M. Imai, K. Yoshimura, and F. M. Grosche, Phys. Rev. Lett. **114**, 097002 (2015).

[12] W. C. Yu, Y. W. Cheung, P. J. Saines, M. Imai, T. Matsumoto, C. Michioka, K. Yoshimura, and S. K. Goh, Phys. Rev. Lett. **115**, 207003 (2015).

[13] P. K. Biswas, Z. Guguchia, R. Khasanov, M. Chinotti, L. Li, K. Wang, C. Petrovic, and E. Morenzoni, Phys. Rev. B **92**, 195122 (2015).

[14] S. Gerber, J. L. Gavilano, M. Medarde, V. Pomjakushin, C. Baines, E. Pomjakushina, K. Conder, and M. Kenzelmann, Phys. Rev. B **88**, 104505 (2013).

[15] E. H. Krenkel, M. A. Tanatar, M. Konczykowski, R. Grasset, E. I. Timmons, S. Ghimire, K. R. Joshi, Y. Lee, L. Ke, S. Chen, C. Petrovic, P. P. Orth, M. S. Scheurer, and R. Prozorov, Phys. Rev. B **105**, 094521 (2022).

[16] K. Ghosh, S. Ramakrishnan, and G. Chandra, Phys. Rev. B **48**, 10435 (1993).

[17] R. Gumeniuk, M. Nicklas, L. Akselrud, W. Schnelle, U. Schwarz, A. A. Tsirlin, A. Leithe-Jasper, and Y. Grin, Phys. Rev. B **87**, 224502 (2013).

[18] O. Prakash, A. Thamizhavel, and S. Ramakrishnan, J. Phys.: Conf. Ser. **592**, 012065 (2015).

[19] O. Prakash, A. Thamizhavel, and S. Ramakrishnan, Supercond. Sci. Technol. **28**, 115012 (2015).

[20] Z. F. Weng, M. Smidman, G. M. Pang, O. Prakash, Y. Chen, Y. J. Zhang, S. Ramakrishnan, and H. Q. Yuan, Phys. Rev. B **95**, 184501 (2017).

[21] O. Prakash, A. Thamizhavel, and S. Ramakrishnan, J. Phys.: Conf. Ser. **568**, 022039 (2014).

[22] R. M. Fleming, A. P. Ramirez, M. J. Rosseinsky, D. W. Murphy, R. C. Haddon, S. M. Zahurak, and A. V. Makhija, Nature (London) **352**, 787 (1991).

[23] K. Holczer, O. Klein, S. Huang, R. B. Kaner, K. Fu, R. L. Whetten, and F. Diederich, Science **252**, 1154 (1991).

[24] J. Nagamatsu, N. Nakagawa, T. Muranaka, Y. Zenitani, and J. Akimitsu, Nature (London) **410**, 63 (2001).

[25] A. Bhattacharyya, D. T. Adroja, N. Kase, A. D. Hillier, A. M. Strydom, and J. Akimitsu, Phys. Rev. B **98**, 024511 (2018).

[26] A. Bhattacharyya, D. T. Adroja, J. Quintanilla, A. D. Hillier, N. Kase, A. M. Strydom, and J. Akimitsu, Phys. Rev. B **91**, 060503(R) (2015).

[27] A. Bhattacharyya, D. T. Adroja, N. Kase, A. D. Hillier, J. Akimitsu, and A. Strydom, Sci. Rep. **5**, 12926 (2015).

[28] Y. Aoki, A. Tsuchiya, T. Kanayama, S. R. Saha, H. Sugawara, H. Sato, W. Higemoto, A. Koda, K. Ohishi, K. Nishiyama, and R. Kadono, Phys. Rev. Lett. **91**, 067003 (2003).

[29] L. Shu, W. Higemoto, Y. Aoki, A. D. Hillier, K. Ohishi, K. Ishida, R. Kadono, A. Koda, O. O. Bernal, D. E. MacLaughlin, Y. Tunashima, Y. Yonezawa, S. Sanada, D. Kikuchi, H. Sato, H. Sugawara, T. U. Ito, and M. B. Maple, Phys. Rev. B **83**, 100504(R) (2011).

[30] A. Maisuradze, W. Schnelle, R. Khasanov, R. Gumeniuk, M. Nicklas, H. Rosner, A. Leithe-Jasper, Y. Grin, A. Amato, and P. Thalmeier, Phys. Rev. B **82**, 024524 (2010).

[31] A. D. Hillier, S. J. Blundell, I. McKenzie, I. Umegaki, L. Shu, J. A. Wright, T. Prokscha, F. Bert, K. Shimomura, A. Berlie, H. Alberto, and I. Watanabe, Nat. Rev. Meth. Primers **2**, 4 (2022).

[32] A. D. Hillier, J. S. Lord, K. Ishida, and C. Rogers, Philos. Trans. R. Soc. A **377**, 20180064 (2019).

[33] R. Kubo, Hyperfine Interact. **8**, 731 (1981).

[34] R. S. Hayano, Y. J. Uemura, J. Imazato, N. Nishida, T. Yamazaki, and R. Kubo, Phys. Rev. B **20**, 850 (1979).

[35] R. Khasanov, H. Luetkens, A. Amato, H.-H. Klauss, Z. A. Ren, J. Yang, W. Lu, and Z. X. Zhao, Phys. Rev. B **78**, 092506 (2008).

[36] G. M. Luke, Y. Fudamoto, K. M. Kojima, M. I. Larkin, J. Merrin, B. Nachumi, Y. J. Uemura, Y. Maeno, Z. Q. Mao, Y. Mori, H. Nakamura, and M. Sigrist, Nature (London) **394**, 558 (1998).

[37] A. D. Hillier, J. Quintanilla, and R. Cywinski, Phys. Rev. Lett. **102**, 117007 (2009).

[38] P. K. Biswas, H. Luetkens, T. Neupert, T. Stürzer, C. Baines, G. Pascua, A. P. Schnyder, M. H. Fischer, J. Goryo, M. R. Lees, H. Maeter, F. Brückner, H.-H. Klauss, M. Nicklas, P. J. Baker, A. D. Hillier, M. Sigrist, A. Amato, and D. Johrendt, Phys. Rev. B **87**, 180503(R) (2013).

[39] V. Grinenko, R. Sarkar, K. Kihou, C. H. Lee, I. Morozov, S. Aswartham, B. Büchner, P. Chekhonin, W. Skrotzki, K. Nenkov, R. Hühne, K. Nielsch, S. L. Drechsler, V. L. Vadimov, M. A. Silaev, P. A. Volkov, I. Eremin, H. Luetkens, and H. H. Klauss, Nat. Phys. **16**, 789 (2020).

[40] Arushi, D. Singh, A. D. Hillier, M. S. Scheurer, and R. P. Singh, Phys. Rev. B **103**, 174502 (2021).

[41] J. A. T. Barker, D. Singh, A. Thamizhavel, A. D. Hillier, M. R. Lees, G. Balakrishnan, D. M. Paul, and R. P. Singh, Phys. Rev. Lett. **115**, 267001 (2015).

[42] D. Singh, M. S. Scheurer, A. D. Hillier, D. T. Adroja, and R. P. Singh, Phys. Rev. B **102**, 134511 (2020).

[43] D. A. Mayoh, A. D. Hillier, G. Balakrishnan, and M. R. Lees, Phys. Rev. B **103**, 024507 (2021).

[44] Arushi, R. K. Kushwaha, D. Singh, A. D. Hillier, M. S. Scheurer, and R. P. Singh, Phys. Rev. B **106**, L020504 (2022).

[45] J. Zhang, Z. F. Ding, K. Huang, C. Tan, A. D. Hillier, P. K. Biswas, D. E. MacLaughlin, and L. Shu, Phys. Rev. B **100**, 024508 (2019).

[46] Y. J. Uemura, *Muon Science: Muons in Physics, Chemistry, and Materials* (IOP, Bristol, UK, 1999).

[47] M. Mandal, A. Kataria, C. Patra, D. Singh, P. K. Biswas, A. D. Hillier, T. Das, and R. P. Singh, Phys. Rev. B **105**, 094513 (2022).

[48] J. Zhang, D. E. MacLaughlin, A. D. Hillier, Z. F. Ding, K. Huang, M. B. Maple, and L. Shu, Phys. Rev. B **91**, 104523 (2015).

[49] M. Weber, A. Amato, F. N. Gygax, A. Schenck, H. Maletta, V. N. Duginov, V. G. Grebinnik, A. B. Lazarev, V. G. Olshevsky, V. Yu. Pomjakushin, S. N. Shilov, V. A. Zhukov, B. F. Kirillov, A. V. Pirogov, A. N. Ponomarev, V. G. Storchak, S. Kapusta, and J. Bock, Phys. Rev. B **48**, 13022 (1993).

[50] A. Maisuradze, R. Khasanov, A. Shengelaya, and H. Keller, J. Phys.: Condens. Matter **21**, 075701 (2009).

[51] E. H. Brandt, Phys. Rev. B **68**, 054506 (2003).

[52] M. Tinkham, *Introduction to Superconductivity*, 2nd ed. (McGraw-Hill, New York, 1996).

[53] F. Gross, B. S. Chandrasekhar, D. Einzel, K. Andres, P. J. Hirschfeld, H. R. Ott, J. Beuers, Z. Fisk, and J. L. Smoth, Z. Phys. B: Condens. Matter **64**, 175 (1986).
[54] T. P. Orlando, E. J. McNiff, S. Foner, and M. R. Beasley, Phys. Rev. B **19**, 4545 (1979).
[55] B. S. Chandrasekhar and D. Einzel, Ann. Phys. (NY) **505**, 535 (1993).
[56] R. Prozorov and R. W. Giannetta, Supercond. Sci. Technol. **19**, R41 (2006).
[57] A. Carrington and F. Manzano, Physica C **385**, 205 (2003).
[58] H. Padamsee, J. E. Neighbor, and C. A. Shiffman, J. Low Temp. Phys. **12**, 387 (1973).
[59] D. C. Johnston, Supercond. Sci. Technol. **26**, 115011 (2013).
[60] P. K. Biswas, G. Balakrishnan, D. McK. Paul, M. R. Lees, and A. D. Hillier, Phys. Rev. B **83**, 054517 (2011).
[61] R. Khasanov, A. Shengelaya, A. Maisuradze, F. La Mattina, A. Bussman-Holder, H. Keller, and K. A. Müller, Phys. Rev. Lett. **98**, 057007 (2007).
[62] D. Singh, J. A. T. Barker, A. Thamizhavel, D. M. Paul, A. D. Hillier, and R. P. Singh, Phys. Rev. B **96**, 180501(R) (2017).
[63] N. Kase, H. Hayamizu, and J. Akimitsu, Phys. Rev. B **83**, 184509 (2011).
[64] M. Sigrist and K. Ueda, Rev. Mod. Phys. **63**, 239 (1991).
[65] J. Garaud and E. Babaev, Phys. Rev. Lett. **112**, 017003 (2014).
[66] S. Maiti and A. V. Chubukov, Phys. Rev. B **87**, 144511 (2013).
[67] D. Pimenov and A. V. Chubukov, Phys. Rev. B **106**, 104515 (2022).